The Crystallography of Metal Halides formed within Single Walled Carbon Nanotubes

J. Sloan[1,2], G. Brown[1,2], S.R. Bailey[1], K.S. Coleman[1], E. Flahaut[1], S. Friedrichs[1], C. Xu[1], M.L.H. Green[1], R.E. Dunin-Borkowski[2], J.L. Hutchison[2], A.I. Kirkland[3] and R.R. Meyer[3]
[1]Inorganic Chemistry Laboratory, University of Oxford, South Parks Road, Oxford, OX1 3QR, U.K.
[2]Department of Materials, University of Oxford, Parks Road, Oxford, OX1 3PH, U.K.
[3]Department of Materials Science, University of Cambridge, Pembroke Street, Cambridge, CB2 3QZ, U.K.

ABSTRACT

The crystal growth behaviour and crystallography of a variety of metal halides incorporated within single walled carbon nanotubes (SWNTs) as determined by high resolution electron microscopy (HRTEM) is described. Simple packed structures, such as the alkali halides form related structures within SWNTs that are integral atomic layers in terms of their thickness. An enhanced HRTEM image restoration technique reveals precise data concerning lattice distortions present in these crystals. More complex structures formed within SWNTs, such as those derived from 3D complex, layered and chain halides form related crystal structures within SWNTs. In narrow (i.e. 1.6nm diameter) SWNTs, these halides form structures that consist of individual 1D polyhedral chains (1D-PHCs) derived from the corresponding bulk halides within SWNTs. In the case of the 3D complex and layered halide structures, the polyhedral chains form with lower co-ordination than in the bulk. Molecular halides also form within SWNTs but these are frequently disordered and do not readily form organised structures within SWNTs.

INTRODUCTION

Single walled carbon nanotubes (SWNTs) are the ultimate discrete porous structures, consisting of individual sp^2 carbon cylinders with lengths in the μm range and diameters varying from *ca.* 1 nm up to *ca.* 4 nm, although the majority (80-90%) exist within a narrow 1.4-1.6nm range. We have been preparing composites from SWNTs using a capillary method [1,2] with a view to modifying their physical properties. A key aspect of this work involved studying the crystal growth of materials formed inside SWNTs which, in most cases leads to 1D crystal growth behaviour that can be related to the bulk structure of the incorporated halide. We have been studying the crystal growth behaviour of a wide variety of metal halides as a function of bulk structure type (Table 1) and have characterised the crystal growth behaviour within SWNTs, using HRTEM imaging, structural modelling and image simulation.

EXPERIMENTAL DETAILS

The nanotubes were produced by a high yield arc synthesis method [3] and then filled in 20-70% yield by the capillary wetting technique [1,2]. The samples were examined at 300 kV in a JEOL JEM-3000F HRTEM, which has a low spherical aberration coefficient C_s of 0.6mm and a point resolution of between 0.16 and 0.17nm. Images were acquired digitally on a Gatan model 794 (1k × 1k) CCD camera, and the magnification was calibrated accurately using Si <110>

lattice fringes. Energy dispersive X-ray microanalysis (EDX) was performed with a LINK 'ISIS' system using a 0.5nm diameter electron probe.

Table 1 Structures of crystalline binary metal halides. The halides indicated in bold have all been prepared inside SWNTs. All the halides other than the molecular halides (which form clusters) form 1D crystals inside SWNTs.

Stoichio-metry	C.N.[a] of M	3D	C.N. of M	Layer	C.N. Of M	Chain	C.N. of M	Mole-cular
MX	4 6 8	Zn Blende **NaCl, AgX** **CsCl, KI**	5+2	TlI (yel.)	2	AuI		
MX_2	4 4 6 6 7 7+2 8	Silica-like ZnI_2 Rutile $CaCl_2$ **SrI_2**, EuI_2 $PbCl_2$ Fluorite	4 6 8	**HgI_2** **(red)** **CdI_2** **$CdCl_2$** **PbI_2** ThI_2	3 3 4 4	$SnCl_2$ GeF_2 $BeCl_2$ $PdCl_2$	2 4	$HgCl_2$ Pt_6Cl_{12}
MX_3	6 7+2 8+1 9	ReO_3-type LaF_3 YF_3 UCl_3, **$LnCl_3$**	6 8+1	YCl_3 BiI_3 $PuBr_3$	4 6	AuF_3 ZrI_3	3 4 4	SbF_3 Al_2Cl_6 Au_2Cl_6
MX_4	6 8 8	IrF_4 ZrF_4 **UCl_4,** **$ThCl_4$**	6 8	PbF_4 ThI_4	5 6 6 6	TeF_4 α- NbI_4 **$ZrCl_4$** **$HfCl_4$**	4 4	$SnBr_4$ **SnI_4**
MX_5	7	β-UF_5			6 6 7	BiF_5 CrF_5 $PaCl_5$	5 6 6	$SbCl_5$ Nb_2Cl_{10} Mo_4F_{20}
MX_6							6	IrF_6

([a]: C.N. = coordination number).

RESULTS AND DISCUSSION

Filling of 1.4nm (*ca.* (10,10)) SWNTs with KI yielded the first example of a rocksalt-type crystal in which all of the atoms are on the surface of the crystal (see Figs. 1(a) and (b)). These crystals image by HRTEM as bilayer arrays of dark spots (Fig. 1(c)). Each dark spot in Fig. 1(c) corresponds to a K-I or a I-K column viewed in projection. As each column consists of the same pair of atoms in projection (ie. either I-K or K-I), the image contrast of all of the columns is identical as verified by image simulations shown in Fig. 1(d) and (e). Tetragonal distortions are present in the bilayer KI crystals. Along the SWNT capillaries, the spots are spaced at regular intervals of *ca.* 0.35nm, conforming to the {200} separation in bulk rocksalt KI, whereas across the SWNT capillary, the separation increases to 0.4nm. These observed distortions could arise as a consequence of two related effects – an interaction between the KI crystal and the tubule wall and the reduced coordination of the atoms compared to the bulk structure (i.e. 4:4 coordination reduced from 6:6).

We have also studied the crystallography of a (3×3) KI crystal formed in wider (12,12) SWNTs using a HRTEM image restoration technique developed in collaboration with Owen Saxton at Cambridge University. From a combined 'through focal' and 'tilt' series of HRTEM images, a phase image is produced that is free of lens aberrations and which is obtained at higher resolution (*ca.* 0.1nm) than conventional HRTEM images (typically 0.16-0.2nm), as shown in Figs. 3(a) and (b). The image restoration and contour map show clearly the positions of all the atoms in the (3×3) crystal as well as indicating the presence of lattice distortions (Fig. 3(c) and (d)).

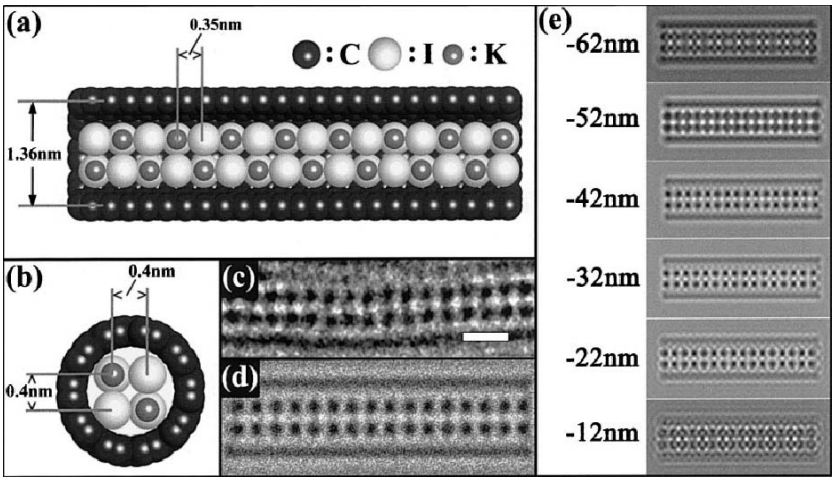

Figure 1 *(a) and (b) cutaway structural representation and end-on view of a (2×2) KI crystal formed inside a SWNT. (c) Experimental HRTEM image of a (2×2) KI crystal. Along the length of the SWNT, the spot spacing corresponds to ~0.35nm, while across the tubule, the spacing increases to ~0.4nm (i.e. as indicated in (a) and (b)). (e) HRTEM image simulation computed for –44nm defocus for an undistorted bilayer KI crystal within a (10,10) SWNT. (e) Calculated HRTEM through focal series of a bilayer crystal within a (10,10) SWNT.*

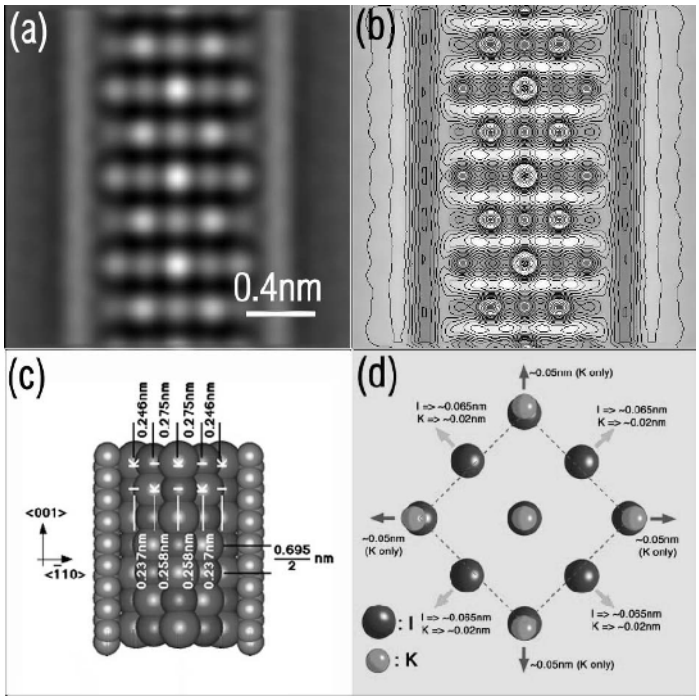

Figure *2(a) Phase image reconstruction of a [110] (i.e. cell diagonal) projection of a 3 layer thick KI crystal. In this projection, all the imaged atoms columns are either pure I or pure K (b) Contour map of phase image (c) Structural model of the KI crystal inside the SWNT showing observed lattice distortions. (d) Unit cell diagram showing individual atomic column displacements in the observed crystal.*

Narrow SWNTs with diameters in the range 1.4-1.6nm can incorporate individual polyhedral chains of metal halides inside SWNTs. By HRTEM these crystals, when viewed in ‘side on’ projection, image as ‘zig-zag’ arrays of dark spots. The dark spots will normally correspond to

the most strongly scattering species in the polyhedral chain. Figure 3 shows two HRTEM images (i.e. Figs (a) and (b)) of $CdCl_2$ formed within 1.4nm (*ca.* (10,10) SWNTs). In this case, most of the contrast within the 'zig-zag' array corresponds to the more strongly scattering Cd^{2+} cation sublattice with the weaker scattering Cl^- anion sublattice being effectively invisible. In Figs. 3(c)-(g), a derivation of the 1D polyhedral chain structure, derived from the bulk layered form of $CdCl_2$ is shown. In effect an individual polyhedral chain of $CdCl_2$ is selected from a single slab of bulk $CdCl_2$. As a chain of lattice terminating $CdCl_6$ octahedra will have a net stoichiometry of $CdCl_3$ (i.e. Fig. 3(d)) it is necessary to remove the terminating – or 'dangling' Cl^- anions in order to produce a net stoichiometry of $CdCl_2$ (i.e. Figs. (e) and (f)). The obtained 1D polyhedral chain is therefore of reduced coordination – effectively square pyramidal (Fig. 3(g)) – compared to the bulk halide (*cf.* (2×2) KI - see above).

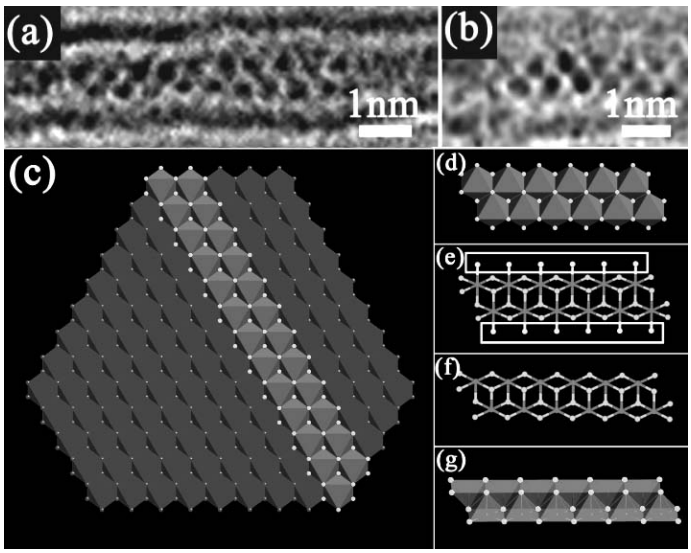

Figure 3*(a) and (b) HRTEM micrographs showing side on views of a 1D polyhedral chain of $CdCl_2$ formed inside a 1.4nm diameter (ca. (10,10)) SWNT. Individual $CdCl_x$ polyhedra image as a 1D 'zig-zag' array of dark spots formed along the SWNT capillaries. (c)-(g) Derivation of a reduced coordination 1D array of edge-linked $CdCl_2$ square pyramids: (c) - bulk $CdCl_2$ structure; (d) 1D chain of '$CdCl_3$' extracted from light grey region in (c); (e) removal of terminal Cls; (f) and (g) 1D polyhedral chain of edge-linked $CdCl_2$ square pyramids.*

Lanthanide (or rare earth) ions have optical and magnetic properties that are particularly interesting when they are situated in a confined geometry. Additionally, as their spectral and dynamic properties alter when the reduced dimensions also affect the chemical and physical properties of the host, these species can act as a local probe for the chemistry and structure of the host material. We have successfully incorporated 1D crystals of these materials into SWNTs as shown by the examples in Figure 4 and 5 [6].

The HRTEM micrograph in Fig. 4(a) shows an example of $TbCl_3$ filling observed within a SWNT bundle. An enlargement of the tubule on the periphery of the bundle (Fig. 1(b)) reveals that the crystal images as a 'zig-zag' array of dark spots which we take to be a chain of $TbCl_6$ polyhedra. Most of the dark contrast in the 1D arrays must originate from the strongly scattering Tb^{3+} centres with the coordinating Cl^- ions being effectively invisible. The bulk structure of $TbCl_3$ normally consists of $TbCl_9$ polyhedra arranged into a 3D hexagonal network (*i.e.* UCl_3-type). Within the confines of the 1.6 nm diameter SWNT in Fig. 4, it is possible only to accommodate 1D polyhedral chains from the 3D structure, as for $CdCl_2$ (see above). The individual polyhedra within the chains are also likely to be of reduced coordination owing to

lattice terminations enforced by capillary confinement and the likeliest candidate structure is

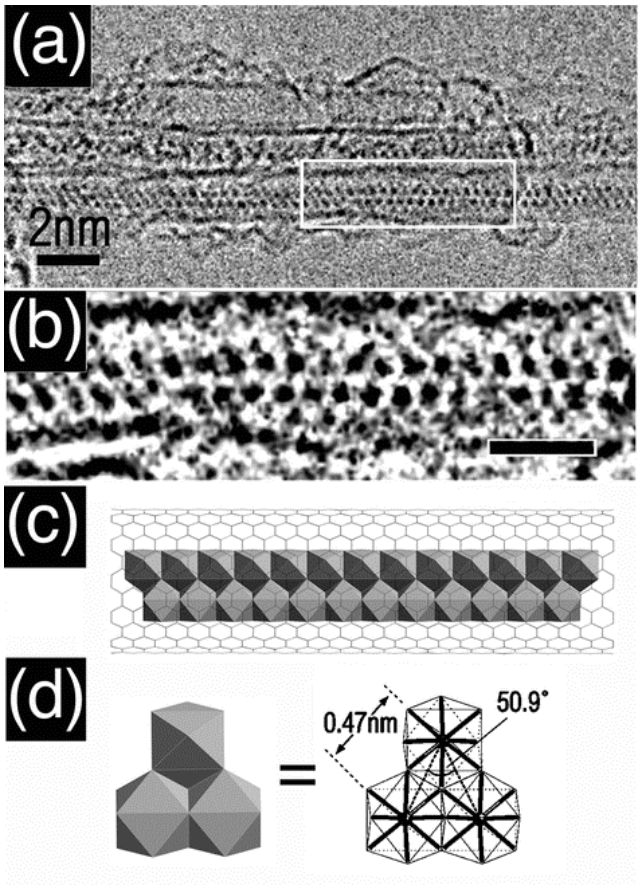

therefore a 1D network of edge-sharing $TbCl_6$ octahedra as depicted in Figs. 4(c) and (d).

Figure 4 *(a) HRTEM image of TbCl3 filling within a SWNT bundle. (b) Enlargement from boxed region in (a) showing a zigzag arrangement of dark spots attributed to a 1D polyhedral chain of TbClx polyhedra (scale bar = 1.6 nm). (c) Structural representation of a 1D polyhedral chain incorporated in a (12,12) SWNT. (d) Detail (left) and schematic depiction (right) of three polyhedra from the encapsulated chain shown in Fig. 1(c). The indicated dimensions in the schematic depiction are estimated from the lattice image [i.e. from (a) and (b)].*

Fig. 5(a) shows a 1D chain of $GdCl_3$ incorporated into a 1.4 nm SWNT. The SWNT is bent into an elbow and, on either side of the bend, the crystal images with different contrast suggesting a different orientation formed as a result of a twist induced by the bend. On the right of the bend, the crystal images as an apparently linear array of dark spots, as can be seen in the enlargement in Fig. 5(b). In this case we assume that the crystal has a similar structure to that depicted in Fig. 4(c) but that it is rotated 90° about the SWNT axis [*i.e*. relative to Fig. 4 (c)] so that the polyhedral chain is viewed in top down projection as depicted in Fig. 5(c). This crystal can also be seem to terminate within the SWNT capillary.

Fig. 5(d) shows a bundle of two SWNTs, one wide (*ca*. 2.5 nm) and the other narrow (*ca*. 1.6 nm), corresponding approximately to (12,12) and (20,20) SWNTs, respectively, both of which are continuously filled with crystalline $NdCl_3$. This crystal has an unusual microstructure as can be seen by the enlargement in Fig. 5(e). The encapsulated crystal consists of two linear 1D arrays of dark spots separated, in the middle, by a continuous series of groups of four dark spots arranged into diamonds. This microstructure cannot readily be reconciled with the bulk structure

of $NdCl_3$, but may instead correspond to the suggested arrangement in Fig. 5(f) in which 'diamond' arrays of $NdCl_x$ polyhedra formed along the centre of the SWNT are bounded by 1D arrays of NdCl*x* polyhedra formed along their walls.

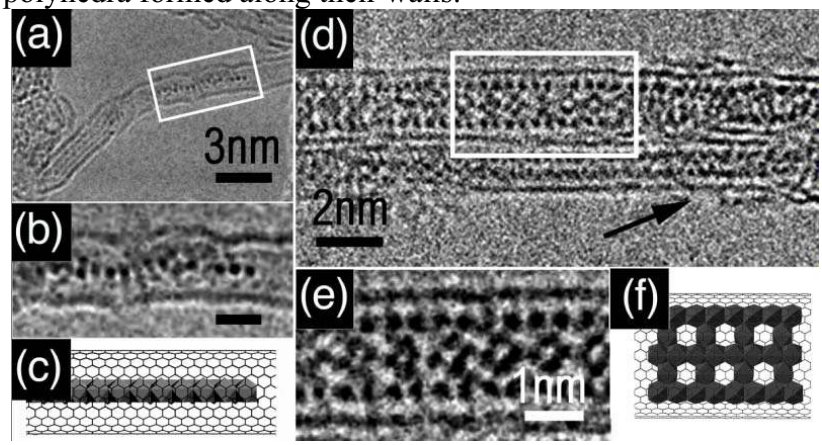

Figure 5 *(a) HRTEM micrograph showing a twisted 1D chain of $GdCl_3$ formed within a (10,10) SWNT. (b) Enlargement of boxed region from (a) showing a linear array of dark spots which terminates towards the right of the micrograph. (d) Structural representation showing a 'top-down' view of a 1D polyhedral chain based on the $CdCl_2$ structure (b) (cf. Fig. 4(d), above)). (d) Bundle consisting of one wide (ca. 2.5nm) and one narrow (arrowed; ca. 1.6nm) SWNT filled with $NdCl_3$. (e) Enlargement of boxed region in (d) showing the unusual microstructure of the $NdCl_3$ filling. (f) Suggested structural model - a 'diamond' array of $NdCl_3$ polyhedra are bounded by 1D polyhedral chains of $NdCl_3$*

ACKNOWLEDGEMENTS

Financial support was provided by Petroleum Research Fund, administered by the American Chemical Society (Grant No. 33765-AC5), the EPSRC (Grant Nos. GR/L59238 and GR/L22324) and Colebrand Ltd. for financial support. S.F. is indebted to BMBF and to the Fonds der Chemischen Industrie for additional financial support. J.S. and E.F. are indebted to the Royal Society.

REFERENCES

1. J. Sloan, D.M. Wright, H.G. Woo, S. Bailey, G. Brown, A.P.E. York, K.S. Coleman, J.L. Hutchison, M.L.H. Green, *Chem. Commun.*, 699 (1999).
2. P. M. Ajayan and S. Iijima, *Nature*, **361**, 333 (1993).
3. C. Journet, W.K. Maser, P. Bernier, A. Loiseau, M. Lamy, M.L. de la Chapelle, S. Lefrant, P. Derniard, J.E. Fisher, *Nature*, **388**, 756 (1997).
4. J. Sloan, M. Novotny, S.R. Bailey, G. Brown, C. Xu, V.C.Williams, S. Freidrichs, E. Flahaut, R.L. Callendar, A.P.E. York, K.S. Coleman and M.L.H. Green, *Chem. Phys. Lett.,* **329**, 61 (2000).
5. R.R. Meyer, J.Sloan, R.E. Dunin-Borkowski, M.C. Novotny, S.R. Bailey, J.L. Hutchison and M.L.H. Green, *Science*, **289**, 1324 (2000).
6. C. Xu, J. Sloan, G. Brown, S. Bailey, V.C. Williams, S. Friedrichs, K.S. Coleman, E. Flahaut, J.L. Hutchison, R.E. Dunin-Borkowski and M.L.H. Green, *Chem. Commun.*, 2427-2428 (2000).